

# Altered default mode network configuration in posttraumatic stress disorder after earthquake

## A resting-stage functional magnetic resonance imaging study

Xiao-Dong Zhang, MD<sup>a</sup>, Yan Yin, MD<sup>b</sup>, Xiao-Lei Hu, MD<sup>c</sup>, Lian Duan, MD<sup>c</sup>, Rongfeng Qi, MD<sup>a</sup>, Qiang Xu, MS<sup>a</sup>, Guang-Ming Lu, MD<sup>a,\*</sup>, Ling-Jiang Li, MD<sup>c,\*</sup>

### Abstract

The neural substrates of posttraumatic stress disorder (PTSD) are still not fully elucidated. Hence, this study is to explore topological alterations of the default mode network (DMN) in victims with PTSD after a magnitude of 8.0 earthquake using resting-state functional magnetic resonance imaging (rs-fMRI).

This study was approved by the local ethical review board, and all participants signed written informed consent. Sixty-two PTSD victims from the 2008 Sichuan earthquake and 62 matched exposed controls underwent rs-fMRI. PTSD was diagnosed by Clinician-Administered PTSD Scale, and underwent PTSD Checklist-Civilian Version for symptom scoring. The DMN was analyzed by using graph theoretical approaches. Further, Pearson correlation analysis was performed to correlate neuroimaging metrics to neuropsychological scores in victims with PTSD.

Victims with PTSD showed decreased DMN functional connectivity strength between the right superior frontal gyrus and left inferior parietal lobule (IPL), and showed increased functional connectivity between the right IPL and precuneus or left posterior cingulate cortex. It was also found that victims with PTSD exhibited decreased nodal efficiency in right superior frontal gyrus and precuneus, and increased nodal efficiency in right hippocampus/parahippocampus. Apart from that, PTSD showed higher nodal degree in bilateral hippocampus/parahippocampus. In addition, the functional connectivity strength between the right IPL and precuneus correlated negatively to the avoid scores ( $r = -0.26$ ,  $P = .04$ ).

This study implicates alteration of topological features on the DMN in PTSD victims after major earthquake, and provides new insights into DMN malfunction in PTSD based on graph theory.

**Abbreviations:** ACC = anterior cingulate cortex, DMN = default mode network, IPL = inferior parietal lobule, PCC = posterior cingulate cortex, PCu = precuneus, rs-fMRI = resting-state fMRI.

**Keywords:** default mode network, earthquake, graph theory, posttraumatic stress disorder, resting-state functional magnetic resonance imaging

Editor: Younbyoung Chae.

This work was supported by the National Natural Science Foundation of China (30830046–81171286 and 91232714 to LL), the National 973 Program of China (2009CB918303 to LL), and a Chinese Key Grant to GL (BWS11J063 and 10z026). The authors declare no conflicts of interest.

Author Contributions: XDZ and YY contributed equally to this work; GML and LJL designed the research. XDZ, YY, XLH, LD, RFQ, QX, GML, and LJL contributed to the writing of the article.

Supplemental Digital Content is available for this article.

<sup>a</sup> Department of Medical Imaging, Jinling Hospital, Medical School of Nanjing University, Nanjing, <sup>b</sup> The Seventh People's Hospital of Hangzhou, Hangzhou, Zhejiang, <sup>c</sup> Mental Health Institute, The Second Xiangya Hospital of Central South University, Hunan, People's Republic of China.

\* Correspondence: Guang-Ming Lu, Department of Medical Imaging, Jinling Hospital, Medical School of Nanjing University, No. 305 Zhongshan East Road, Nanjing 210002, Jiangsu Province, People's Republic of China (e-mail: gjr.luguangming@vip.163.com); Ling-Jiang Li, Mental Health Institute, The Second Xiangya Hospital of Central South University, 139# Renmin Zhong Road, Changsha 410011, Hunan, People's Republic of China (e-mail: llj2920@163.com).

Copyright © 2017 the Author(s). Published by Wolters Kluwer Health, Inc. This is an open access article distributed under the terms of the Creative Commons Attribution-Noncommercial License 4.0 (CCBY-NC), where it is permissible to download, share, remix, transform, and buildup the work provided it is properly cited. The work cannot be used commercially without permission from the journal.

Medicine (2017) 96:37(e7826)

Received: 20 April 2017 / Received in final form: 28 July 2017 / Accepted: 31 July 2017

<http://dx.doi.org/10.1097/MD.0000000000007826>

## 1. Introduction

Posttraumatic stress disorder (PTSD) is a severe anxiety disorder that is implicated with the exposure to life-threatening traumatic events.<sup>[1]</sup> PTSD could affect multiple domains of health. Three symptom clusters (ie, hyperarousal, re-experiencing, and avoidance) are most prominent and are considered as therapeutic focus.<sup>[2]</sup> These symptoms could cause persistent harm to personal health, compromise the quality of life, and might induce disabling conditions.<sup>[3]</sup> Understanding the neurophysiological mechanism underlying PTSD could be of benefit to the therapy. Nonetheless, the neural substrates of PTSD are still not fully elucidated.

Plenty of studies indicated aberrant internally focused thought and function of autobiographical memory in patients with PTSD, which implied malfunction of the default mode network (DMN). The DMN is probably the most intensively studied resting-state brain network, which is composed of a series of brain regions anticorrelated with the frontoparietal network, and exhibits hyperactivity at rest and hypoactivity in the presence of attention-demanding tasks.<sup>[4]</sup> The DMN could be considered as a state ready to respond to any outside challenges.<sup>[5]</sup> Apart from the widely known functions of the DMN such as self-reflection and self-awareness, studies have also linked clinical manifestations of PTSD to perturbed functional connectivity of the DMN at resting state.<sup>[6,7]</sup>

Lines of evidences have proved that compromised integrity of the DMN might be possible neural substrate in the etiology of PTSD.<sup>[6–8]</sup> Bluhm et al<sup>[6]</sup> first studied the alteration of resting-state functional connectivity of DMN in female patients with

childhood abuse by using seed-based correlation analysis. Lanius et al<sup>[7]</sup> further found that the altered functional connectivity of the DMN could predict the severity of PTSD. By using similar ROI-based functional connectivity analysis, Sripatha et al<sup>[9]</sup> studied both the DMN and salient network, and found the disequilibrium between these 2 networks in PTSD. In another seed-based DMN study, King et al<sup>[10]</sup> found increased functional connectivity between posterior cingulate cortex (PCC) and dorsal lateral prefrontal cortex, and between PCC and dorsal anterior cingulate cortex after mindfulness-based exposure therapy in combat veterans with PTSD. Apart from seed-based or ROI-based analysis, independent component analysis (ICA) was also widely implemented in DMN functional connectivity investigation with the advantage of bias-free concurrent multi-network analysis. Tursich et al<sup>[11]</sup> utilized ICA to assess the association between spontaneous activity of the DMN, salience network and central executive network, and PTSD symptom severity in distinct symptom clusters. In their study, function of the DMN was altered and correlated to depersonalization/derealization severity in PTSD. Recently, topological large-scale network analysis based on graph theory is making rapid and wide progress in neuroscience and clinical contexts,<sup>[12]</sup> which provides a way to assess both the local and distant functional connectivity organization of the brain networks. Moreover, this method is a data driven methodology for whole brain network analyses without priori ROI or seed selection. By using this topological method, Lei et al<sup>[13]</sup> found the topological features of PTSD shifted to “small-worldization” and the disequilibrium between the DMN and the salience network. Further, Du et al<sup>[8]</sup> found persistent connectivity malfunction belonged to the DMN in major earthquake survivors after 2 years, indicating a long-term effect of earthquake on this important human brain network. Kennis et al<sup>[14]</sup> indicated that DMN regions had reduced degree in PTSD, but an increased degree in the PCu. Suo et al<sup>[15]</sup> found that the main increased nodal activities were within the DMN in pediatric PTSD patients. Nonetheless, these studies investigated the DMN in the context of the whole resting brain network, and no study has further concentrated the attention on the alteration of topological organization in the DMN of PTSD as a separate brain network. We therefore try to exclusively construct DMN of PTSD with the predefined nineteen nodes for the brain network construction related with DMN. By doing this, more detailed information of altered brain network features might be uncovered. In addition, the DMN could also be considered as a brain network and studies have found topological reorganization of the DMN in mild cognitive impairment<sup>[16]</sup> and irritable bowel syndrome.<sup>[17]</sup> Thus, It seems plausible that the topological organization of the DMN would also be altered in victims with PTSD after the major earthquake. Our study is the first one to assess the topological traits of the DMN in earthquake survivors, by exclusively constructing the DMN with the predefined seeds. In addition, we further correlate the neuroimaging metrics to the neuropsychological tests scores of PTSD.

## 2. Materials and methods

### 2.1. Participants

This study was approved by the local ethical committee. Written informed consents were obtained before the study from all participants who were victims from an eight-magnitude earthquake on May 12, 2008 in Sichuan Province, China. A screening PTSD survey was conducted first by using PTSD Checklist-Civilian

Version (PCL-C).<sup>[18]</sup> Then, Clinician-Administered PTSD Scale (CAPS)<sup>[19]</sup> was further implemented to score the symptom severity. This study used a PCL cut off of 35 to trigger screening with the CAPS followed by inclusion with CAPS score >50.<sup>[20]</sup> The diagnosis of PTSD was established according to Structured Clinical Interview for DSM-IV axis I Disorders (SCID-I).<sup>[21]</sup> Victims consequently (9–16 months after the earthquake) underwent rs-fMRI examinations, and the inclusion criteria were listed as follows: ① victims with PTSD and in the absence of any other psychiatric disorders according to SDIC-I; ② right handed; ③ younger than 60 years. The exclusion criteria were: ① any psychiatric comorbidity or psychiatric history; ② head trauma or loss of consciousness; ③ drug, psychiatric medication or alcohol usage; ④ brain tumors, hemorrhage, infarction and severe neural degeneration; ⑤ MRI contraindications (such as claustrophobia). Seventy-two cases of victims with PTSD (PTSD group) accomplished the examination and all MRI data sets were collected. In addition, 86 cases of age, sex, and education level matched victims without PTSD (non-PTSD group) were recruited and also underwent the same MRI protocol. The inclusion and exclusion criteria for non-PTSD group were identical to the PTSD group, except for the exclusion diagnosis of PTSD. Further, based on the head motion parameters, we excluded the victims in both groups with head translation more than 2mm or rotation more than 2° during MR scanning. 62 cases of PTSD and 62 cases of non-PTSD were finally enrolled in this rs-fMRI study.

### 2.2. Rs-MRI acquisition

All the rs-MRI data were collected by using 3 Tesla MR scanner (EXCITE, General Electric, Milwaukee) with an 8-channel phased-array head coil. Participants of PTSD and non-PTSD groups were instructed to keep awake with eyes closed and not to think anything particular during the rs-fMRI scanning. Foam pads were used to constrain the involuntary head motion of all participants. Besides, earplugs were applied for hearing protection. A gradient-recalled echo planar imaging MRI sequence was performed along the anterior commissure–posterior commissure line. The parameters of this MRI sequence were: repetition time (TR)=2000 ms, echo time (TE)=30 ms, field of view (FOV)=220 × 220 mm<sup>2</sup>, flip angle=90°, matrix=64 × 64, slice thickness=3 mm, slice gap=1 mm. Each brain contained 30 slices. For each participant, 200 brain volumes were acquired with time cost of 400 s.

### 2.3. Data Preprocessing

Statistical parametric mapping (SPM8, <http://www.fil.ion.ucl.ac.uk/spm/>) based on MATLAB (The Math Works, Inc., Natick, MA) platform was used to preprocess functional MRI data. First, the first 10 time points were excluded for the signal homogeneity and participants' adaptation to the scanning. Second, slice timing correction was performed to compensate the temporal difference between slices. Third, head motion was corrected to rule out subjects with head motion more than 2mm translation in any axis or more than 2° rotation in any axis during data acquisition. Moreover, according to the formula provided by Liao et al,<sup>[22]</sup>

$$\text{head motion} = \frac{1}{L-1} \sum_{i=2}^L \sqrt{(x_i - x_{i-1})^2 + (y_i - y_{i-1})^2 + (z_i - z_{i-1})^2}$$

we compared the differences of translation and rotation between the 2 groups. No statistical difference was found (2-sample *t* test, translation *t*=0.283, *P*=.792; rotation *t*=0.254,

$P = .792$ ).  $L$  denotes the length of the acquisition time ( $L = 200$  in this study).  $x_i$ ,  $y_i$ , and  $z_i$  represents translations/rotations at the  $i$ th time point in the  $x$ ,  $y$ , and  $z$  directions, respectively. Fourth, functional maps were spatially normalized to the standard Montreal Neurological Institute (MNI) EPI template with a resampled voxel size of  $3 \times 3 \times 3 \text{ mm}^3$ . Fifth, detrending was performed to remove the linear trend of time courses. Sixth, low-pass filtered (0.01–0.08 Hz) was done to reduce the effects of noises. Seventh, global signal,<sup>[23]</sup> white matter signals, cerebrospinal fluid signals, and head motion parameters were removed as nuisance signals by linear regression. Eighth, all the functional data was spatially smoothed with an isotropic Gaussian kernel of 8 mm full-width at half-maximum (FWHM) by using SPM8.

#### 2.4. Nodes of DMN in both groups

Default mode network for further fMRI analysis was constructed by using a published atlas of region of interests (ROIs) released by functional imaging in neuropsychiatric disorders (FIND) laboratory of the Stanford University ([http://findlab.stanford.edu/functional\\_ROIs.html](http://findlab.stanford.edu/functional_ROIs.html)). This ROI atlas was defined from a group-level independent component analysis of resting-state fMRI.<sup>[24]</sup> We excluded ROIs situated on thalamus, middle cingulate cortex and cerebellum as these locations were considered not typical for DMN.<sup>[25]</sup> Nineteen ROIs were considered as nodes or seeds for further functional connectivity and network analysis (Table 1). (See supp Figure 1, <http://links.lww.com/MD/B863>, Supplemental Content, which illustrates the ROIs selected in this study).

#### 2.5. Edges of DMN in both groups

Average signal of time series in each ROI was extracted for further functional connectivity analysis. Pearson correlation coefficients were calculated between each pair of 19 nodal time series for functional connectivity analysis in each participant. Then, a square  $19 \times 19$  correlation matrix was constructed.

**Table 1**  
The DMN nodes released by FIND laboratory.

Number	ROIs defined by FIND	Abbreviations
1	Dorsal DMN 01	mPFC/ACC
2	Dorsal DMN 02	IPL-BA39-L
3	Dorsal DMN 03	SFG-R
4	Dorsal DMN 04	PCu-BA31
5	Dorsal DMN 06	IPL-BA39-R
6	Dorsal DMN 08	H/PH-L
7	Dorsal DMN 09	H/PH-R
8	Precuneus 02	PCu-BA7-dorsal
9	Precuneus 03	IPL-BA40-L
10	Precuneus 04	IPL-BA40-R
11	Ventral DMN 01	PCC-L
12	Ventral DMN 02	MFG/SFG-L
13	Ventral DMN 03	Fusiform-L
14	Ventral DMN 04	OMG-L
15	Ventral DMN 05	PCC-R
16	Ventral DMN 06	PCu-BA7-vertral
17	Ventral DMN 07	MFG/SFG-R
18	Ventral DMN 08	Fusiform-R
19	Ventral DMN 09	OMG-R

BA = Brodmann Area, DMN = default mode network, FIND = functional imaging in neuropsychiatric disorders, H/PH = hippocampal/parahippocampal, IPL = inferior parietal lobule, L = left, MFG = middle frontal gyrus, mPFC/ACC = medial prefrontal lobule/anterior cingulate cortex, OMG = middle occipital gyrus, PCC = posterior cingulate cortex, PCu = precuneus, R = right, ROI = region of interest, SFG = superior frontal gyrus.

Afterwards, all correlation coefficients were converted to  $z$  values by using Fisher  $r$ -to- $z$  transformation to make the data normally distributed which would facilitate the following statistical analysis. For a weighted network,  $z$  values denote the functional connectivity strength between each pair of nodes. Each pair of functional connectivity was considered as an edge in this sub-network. In this study, 171 ( $C_{19}^2 = 171$ ) possible edges along with 19 nodes constructed the DMN.

#### 2.6. Network analysis of DMN

We used Graph theoRETical Network analysis (GRETNA) toolbox (<http://www.nitrc.org/projects/gretna/>) to evaluate the topological organization of the DMN in PTSD.<sup>[26]</sup> In this study, we mainly discussed the network efficiency, small world properties, nodal efficiency and nodal degree (ie, nodal degree in recent study) based on graph theory.

Specifically, in a brain network ( $G$ ), sparsity<sup>[27]</sup> is defined as the ratio of the existing number of edges to the number of all possible edges in the network ( $C_{19}^2 = 171$  in the present study). Network efficiency<sup>[28]</sup> is calculated by the  $E(G) = \frac{1}{N_G(N_G-1)} \sum_{i \neq j \in G} \frac{1}{d_{ij}}$ , where  $d_{ij}$  denotes the shortest path length between nodes  $i$  and  $j$ . When  $G$  represents a whole network (the DMN in this study),  $E(G)$  reflects the global efficiency ( $E_{\text{glob}}$ ) and  $N_G$  denotes the number of nodes in the whole network. Although  $G$  is a sub-network,  $E(G)$  means the local efficiency, ( $E_{\text{loc}}$ ) and  $N_G$  is the number of nodes in the sub-network.  $E_{\text{glob}}$  and  $E_{\text{loc}}$  are important metrics for assessing the ability of global and local information transmission in a brain network. In physiological conditions, human brain network would keep a balance over  $E_{\text{glob}}$  and  $E_{\text{loc}}$ , which might be disrupted in pathological circumstances.<sup>[29]</sup>

Three parameters are used to characterize the small world properties, including  $\gamma$ ,  $\lambda$ , and  $\sigma$ . Compared with random networks, small-world networks yield similar path lengths but higher clustering coefficients, characterized by  $\gamma = C_p^{\text{real}}/C_p^{\text{rand}} \gg 1$  and  $\lambda = L_p^{\text{real}}/L_p^{\text{rand}} \approx 1$ ,<sup>[30]</sup> or by using small-worldness,<sup>[31]</sup>  $\sigma = \gamma/\lambda > 1$ .  $C_p^{\text{real}}$  and  $C_p^{\text{rand}}$  denotes clustering coefficients in real network and random network respectively.  $L_p^{\text{real}}$  and  $L_p^{\text{rand}}$  represents path length of real network and random network respectively.

For a weighted network  $G$  with  $N$  nodes, the nodal efficiency could be computed by the following formula<sup>[32]</sup>:  $E_{\text{nodal}}(i) = \frac{1}{N-1} \sum_{i \neq j \in G} \frac{1}{L_{ij}}$ .  $E_{\text{nodal}}(i)$  denotes nodal efficiency of the  $i$ th node. Nodal degree is  $S_p(G) = \frac{1}{N} \sum S(i)$ , where  $S(i)$  denotes the number of edges of the  $i$ th node.<sup>[33]</sup> In this study, nodal efficiency and degree are the average value of all nodes in the DMN.

#### 2.7. Statistical processes

All the demographic data was compared by using SPSS 20.0 (IBM Inc. Armonk, NY). Independent two sample  $t$  tests were implemented to compare the age and education level in PTSD and non-PTSD groups. Although  $\chi^2$  test was used for comparison of sex. Statistic significant level was set at  $P < .05$ .

All the rs-fMRI maps were processed by using SPM8 (statistical parametric mapping, <http://www.fil.ion.ucl.ac.uk/spm/>). A random-effects 2-sample  $t$  test was performed to evaluate the alteration of functional connectivity (ie, edges) between the 2 groups with age, sex, education level as covariates. False-positive adjustment (FPA) was implemented for multiple comparison correction.<sup>[34]</sup> As 171 possible edges existed in this study, we controlled for the probability of type I error for the

**Table 2****The demographic and neuropsychological data in PTSD and non-PTSD.**

	PTSD (n=62)	Non-PTSD (n=62)	P
Sex (male/female)	17/45	14/48	.53*
Age (yrs, mean±SD)	41.77±8.40	42.10±9.24	.90**
Education level (years, mean±SD)	7.47±2.64	7.53±3.05	.54**
Total CAPS (score)	65.47±12.21	N/A	N/A
Re-experiencing (score)	20.23±5.43	N/A	N/A
Avoidance (score)	23.40±6.68	N/A	N/A
Hyper-arousal (score)	21.79±4.90	N/A	N/A

CAPS=Clinician-Administered PTSD Scale.

\* $\chi^2$  test for sex comparison between two groups.\*\*2-sample *t* test for age and education between 2 groups.

N/A=not applicable.

number of comparisons between the 2 groups ( $P$  value  $< 1/171 = .00584$ ). Further, on the level of each sparsity ( $0.05 \leq \text{sparsity} \leq 0.4$ ), we used 2 sample *t* tests for comparisons of network topological traits between the 2 groups including  $E_{\text{glob}}$ ,  $E_{\text{loc}}$ ,  $\gamma$ ,  $\lambda$ ,  $\sigma$ ,  $E_{\text{nodal}}$ ,  $S_p(G)$  with age, sex, education level as covariates. The significant level was set at  $P < .01$ . In addition, to assess the correlation between the CAPS scores and internodal connectivity/network topological metrics in PTSD victims, we correlated the mean  $z$  values of functional connectivity and values of topological metrics that demonstrated significant difference between the 2 groups against the CAPS scores by using Pearson correlation analysis. Pearson correlation analysis was carried out by using SPSS 20.0 (IBM Inc. Armonk, NY) with a significance level of  $P < .05$ , corrected for multiple comparison by using the false discovery rate correction.

### 3. Results

#### 3.1. Demographic and neuropsychological data

No statistical significance was found in age, education level and sex of the 2 groups (all  $P > .05$ ). The detailed comparisons and neuropsychological data were exhibited in Table 2.

#### 3.2. Altered functional connectivity strength of the DMN

Compared with non-PTSD, victims with PTSD showed decreased functional connectivity strength between right superior frontal

gyrus and left IPL-BA39, whereas increased functional connectivity strengths were found between right IPL-BA40 and PCu-BA31 or left PCC (Fig. 1). (See supp Table 1, <http://links.lww.com/MD/B863>, Supplemental Content, which illustrates FC strength alteration within DMN in PTSD compared with non-PTSD).

#### 3.3. Altered DMN topological features

In both PTSD and non-PTSD groups, the DMN showed small world properties ( $0.05 \leq \text{sparsity} \leq 0.4$ ), characterized by  $\gamma = C_p^{\text{real}}/C_p^{\text{rand}} \gg 1$  and  $\lambda = L_p^{\text{real}}/L_p^{\text{rand}} \approx 1$ , or  $\sigma = \gamma/\lambda > 1$  (see supp Figure 2, <http://links.lww.com/MD/B863>, Supplemental Content, which illustrates small world properties of DMN in PTSD and non-PTSD). We also compared the global and local network efficiency of the DMN (ie,  $E_{\text{glob}}$  and  $E_{\text{loc}}$ ) (see supp Figure 3, <http://links.lww.com/MD/B863>, Supplemental Content, which illustrates global and local efficiency in both groups). However, clustering coefficient and path length,  $\lambda$ ,  $\gamma$ ,  $\sigma$ ,  $E_{\text{glob}}$ , and  $E_{\text{loc}}$  demonstrated no significant difference between PTSD and non-PTSD groups (see supp Table 2, <http://links.lww.com/MD/B863>, Supplemental Content, which illustrates comparison of DMN network metrics between PTSD and non-PTSD).

In terms of the nodal characters of the DMN, victims with PTSD exhibited decreased nodal efficiency in the right superior frontal gyrus ( $0.23 \leq \text{sparsity} \leq 0.3$ ) and the PCu-BA7-vertral ( $0.22 \leq \text{sparsity} \leq 0.28$ ), and increased nodal efficiency in the right H/PH ( $0.18 \leq \text{sparsity} \leq 0.22$ ) compared with

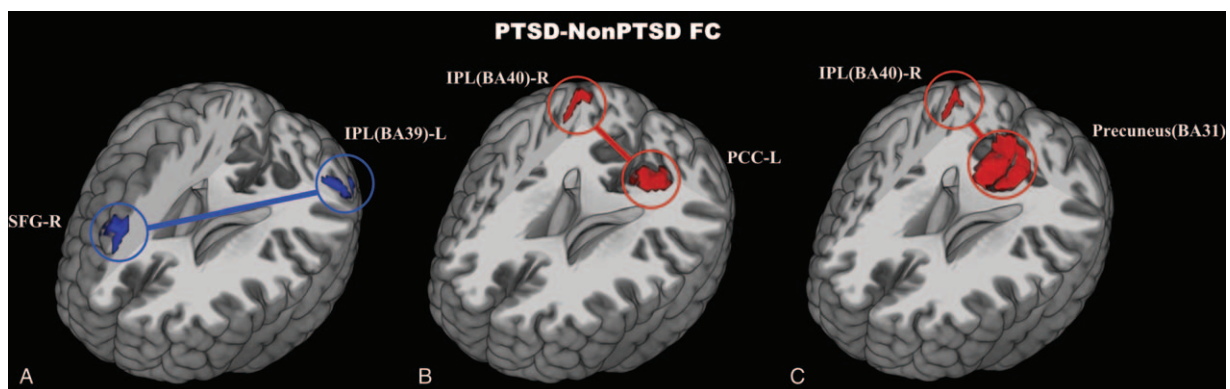


**Figure 1.** Decreased (blue) and increased (red) functional connectivity of DMN in PTSD compared with non-PTSD. FPA correction,  $P < .005$ . BA = Brodmann Area, FC = functional connectivity, FPA = false-positive adjustment, IPL = inferior parietal lobule, Non-PTSD = non-posttraumatic stress disorder, PCC = posterior cingulate cortex, PCu = precuneus, PTSD = posttraumatic stress disorder, SFG = superior frontal gyrus.

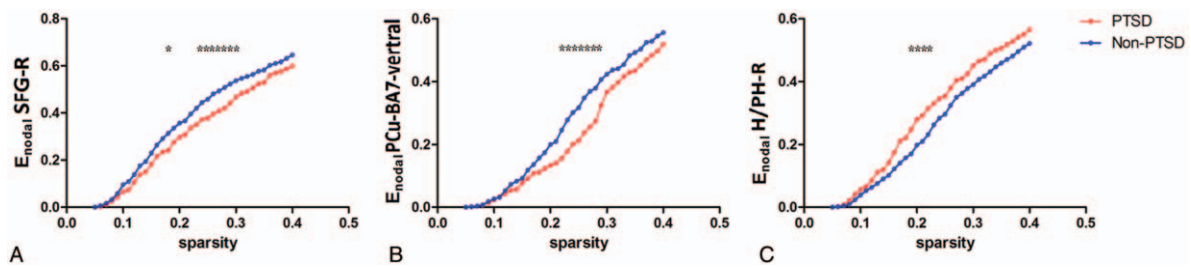


**Figure 2.** Nodal efficiency comparison between PTSD and non-PTSD, significant level  $P < .01$ . Victims with PTSD showed decreased nodal efficiency in right SFG and PCu-BA7-vertral, and increased nodal efficiency in right H/PH compared with non-PTSD. (\* denote significant differences between the 2 groups). BA= Brodmann Area, H/PH=hippocampus/parahippocampus, Non-PTSD=nonposttraumatic stress disorder, PCu=precuneus, PTSD=posttraumatic stress disorder, SFG=superior frontal gyrus.

non-PTSD (Fig. 2). Apart from that, PTSD showed higher nodal degree in the left H/PH ( $0.08 \leq \text{sparsity} \leq 0.14$ ) and the right H/PH ( $0.22 \leq \text{sparsity} \leq 0.34$ ) compared with non-PTSD ( $P < .01$ ).

**3.4. Pearson correlation between imaging parameters and neuropsychological metrics**

Pearson analysis found negative correlation between functional connectivity strength (between right IPL-BA40 and PCu-BA31) and avoidance score ( $P < .05$ ) (Fig. 4). No significant correlation was found between functional connectivity strength, and re-experiencing and hyper-arousal scores. In addition, no significant correlation was found between any investigated topological feature of DMN in PTSD and the scores of the 3 main symptoms.

**4. Discussion**

In the current study, to our knowledge, topological organization of the DMN in victims with PTSD after a major earthquake was analyzed for the first time. Compared with non-PTSD, we found altered functional connectivity strength, nodal efficiency and nodal degree in victims with PTSD, indicating a disturbance in the integration of DMN in PTSD. In addition, we also found negative correlation between functional connectivity strength (between right IPL and PCu) and avoidance score. These findings indicated that, as predicted, topological configuration of the DMN in victims with PTSD after major earthquake was changed, and the alteration was likely to be potential neurophysiological mechanism underlying PTSD.

**4.1. Alteration of inter-seed functional connectivity strength of the DMN in PTSD**

Compared with non-PTSD, survivors with PTSD showed decreased functional connectivity strength between left IPL (BA39) and right superior frontal gyrus. IPL (BA39) is overlapped with angular gyrus. This finding is in line with previous studies that PTSD presented decreased functional connectivity within the DMN.<sup>[35]</sup>

On the contrary, compared with non-PTSD, survivors with PTSD showed increased functional connectivity strength between right IPL (BA40) and PCu (BA31) and increased functional connectivity strength between right IPL (BA40) and left PCC. PCu and PCC are highly connected and metabolic brain regions at resting state, and play a key role in the DMN.<sup>[36]</sup> These properties make PCu and PCC susceptible to functional malformation in the PTSD, indicating these brain regions a potential sensitive biomarker. IPL allows visospatial information processing and relates to body defense, alarming and survival,<sup>[37]</sup> which might also play a vital role in PTSD. The increased functional connectivities in these DMN regions were not reported in any prior study (adult cohort). This finding might attribute to reorganization of brain network and different method used from previous studies. Specifically, we speculated that these increased intra-DMN functional connectivities might play a compensate role in the brain network reorganization. Moreover, we found negative correlation between functional connectivity strength (between right IPL and PCu) and avoidance score, which adds to the proposal of network reorganization aforementioned. The negative correlation might indicate that patients with less severe symptom would allow more compensation for the reduced functional connectivity. Negative correlation between functional

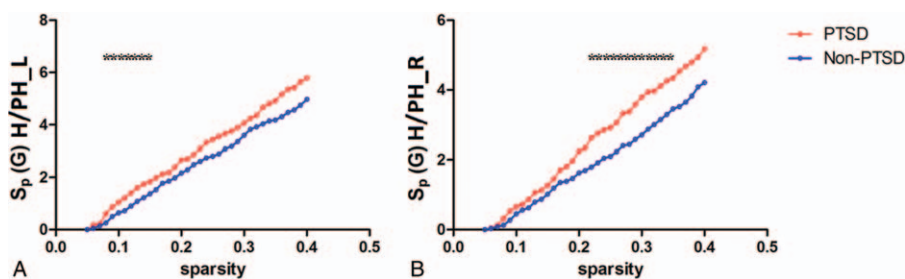


**Figure 3.** Nodal degree comparison between PTSD and non-PTSD, significant level  $P < .01$ . PTSD showed higher nodal degree in bilateral H/PH compared with non-PTSD. (\* denote significant differences between the 2 groups). H/PH=hippocampus/parahippocampus, PTSD=posttraumatic stress disorder, Non-PTSD=nonposttraumatic stress disorder.

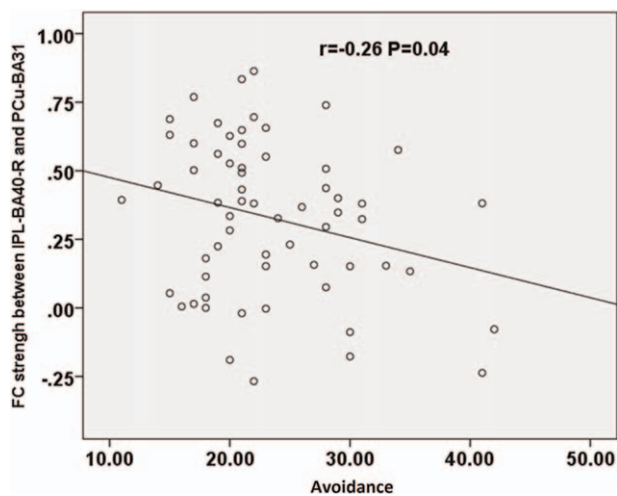


**Figure 4.** Correlation between the score of avoidance and FC strength ( $P < .05$ ). The FC strength between right IPL (BA40) and PCu (BA31) correlate negatively to avoidance score. FC=functional connectivity, IPL=inferior parietal lobule, PCu=precuneus.

connectivity (between the right amygdale and the left middle frontal cortex) and CAPS scores has been reported previously,<sup>[20]</sup> which indicated the impairment of cortex-limbic circuit. However, the exact neural mechanism of the relationship between increased functional connectivity (between right IPL and PCu, 2 highly connected parietal structures) and the PTSD symptom severity remains unknown.

#### 4.2. Alteration of topological features of the DMN in PTSD

According to graph theory, human brain is a complex network with numerous nodes and edges, and possesses small world properties, which allows effective information transfer at low cost.<sup>[26]</sup> In conditions of neuropsychiatric diseases, the topological features of brain network might be altered. In this study, we used graph theory methods to identify the possible topological disturbance of DMN in PTSD by constructing the DMN with the predefined ROIs.

We found that the DMN in PTSD exhibited a trend to small-world brain network ( $\gamma = C_p^{\text{real}}/C_p^{\text{rand}} \gg 1$  and  $\lambda = L_p^{\text{real}}/L_p^{\text{rand}} \approx 1$ ). Generally, the brain network normally functions as a small-world network with a high local specialization and global integration, whereby the brain could run effectively with relatively low energy costs. In a previous study, Lei et al<sup>[13]</sup> defined the whole brain network of PTSD patients with 90 nodes, and found PTSD patients showed a shift to small-world network rather than random network. Thus, it was implied that not only the whole brain network but also the DMN keep the energy-saving topological feature of small world. Moreover, no significant differences of clustering coefficient and characteristic path length were found in the DMN. In addition, no significant differences of the normalized metrics such as  $\gamma$  (normalized clustering coefficient),  $\lambda$  (normalized characteristic path length), and  $\sigma$  ( $\sigma = \gamma/\lambda$ , small-worldness) of the DMN were found between PTSD and non-PTSD groups in our study. These findings were similar to Lei's whole brain topological analysis.<sup>[13]</sup> They found no difference of in the normalized metrics such as  $\gamma$ ,  $\lambda$ , and  $\sigma$  between PTSD and control groups in the whole brain network.<sup>[13]</sup> What's more,  $E_{\text{glob}}$  (global effect) and  $E_{\text{loc}}$  (local

effect) were reduced when considering the whole brain as a network in PTSD,<sup>[13]</sup> whereas they showed no difference in DMN between PTSD and non-PTSD groups in our investigation. According to this clue, we speculated that a mechanism of reorganization might exist to maintain the hyperactive function of DMN in adult PTSD. Apart from the study of adult PTSD, Suo et al<sup>[15]</sup> assessed the whole brain network, and found a significantly increased clustering coefficient, normalized characteristic path length, and  $E_{\text{loc}}$  in pediatric patients with PTSD, which was different with our findings. The possible reasons might be the different ROI selection and different study population.

Apart from investigation of the global topologies of DMN, we also found altered nodal efficiency and degree of the DMN between the two groups. Compared with non-PTSD group, victims with PTSD exhibited decreased nodal efficiency in right superior frontal gyrus and PCu. A recent meta analysis<sup>[38]</sup> of neuroimaging studies on PTSD after natural disasters found perturbed function in right superior frontal gyrus. Superior frontal gyrus is part of prefrontal cortex, which is a key brain region of neural circuit underpinning PTSD, apart from amygdale and hippocampus. Decreased nodal efficiency in right superior frontal gyrus might be related to impaired prefrontal cortex-amygdala neural circuit in PTSD victims, which results in lower top-down control over the activation of amygdala. Decreased nodal efficiency in PCu indicates lower information processing in this key brain region belongs to the DMN.

Notably, we also found increased nodal efficiency in right hippocampus/parahippocampus and higher nodal degree in bilateral hippocampus/parahippocampus in PTSD victims. The hippocampus plays pivotal role in typical neural circuit in the etiology of PTSD,<sup>[39]</sup> and is related to conditioned fear, extinction, and a key mediator of learned fear. Parahippocampus is involved in scene perception, which could be important for human to process information from the surrounding environment during natural disasters such as a major earthquake.<sup>[38]</sup> Most structural MRI studies found decreased hippocampus/parahippocampus volume in PTSD,<sup>[40]</sup> however, the activities of hippocampus/parahippocampus were various by using BOLD fMRI studies.<sup>[41,42]</sup> One account for increased hippocampus/parahippocampus nodal efficiency and degree in this study, might line in a compensatory mechanism. Taken together, these results were in favor of the hypothesis that the topological configuration of the DMN in PTSD victims is altered.

#### 4.3. Limitations

There are some limitations in this study. First, we only studied PTSD caused by one kind of natural disaster, and the result interpretation should not be generalized to other traumatic events. Second, as a cross-sectional study, we can't tell the causality between these topological alterations and PTSD, longitudinal studies are warranted in the future. Third, the data was acquired in the year 2008, so we only assessed three main manifestations of PTSD in line with DSM-IV. As time goes on, 4 main manifestations are introduced by DSM-V.

#### 5. Conclusion

In conclusion, these findings speak to alteration of topological features on the DMN in PTSD victims after major earthquake. This study provides new insights into the DMN malfunction in PTSD based on graph theory.

## Acknowledgments

The authors would like to thank Chang Feng Jin for the assistance with the data acquisition.

## References

- [1] Miller MW, Sadeh N. Traumatic stress, oxidative stress and post-traumatic stress disorder: neurodegeneration and the accelerated-aging hypothesis. *Mol Psychiatry* 2014;19:1156–62.
- [2] Kearney DJ, Simpson TL. Broadening the approach to posttraumatic stress disorder and the consequences of trauma. *JAMA* 2015;314:453–5.
- [3] Admon R, Milad MR, Hendler T. A causal model of post-traumatic stress disorder: disentangling predisposed from acquired neural abnormalities. *Trends Cogn Sci* 2013;17:337–47.
- [4] Anticevic A, Cole MW, Murray JD, et al. The role of default network deactivation in cognition and disease. *Trends Cogn Sci* 2012;16:584–92.
- [5] Raichle ME, Gusnard DA. Intrinsic brain activity sets the stage for expression of motivated behavior. *J Comp Neurol* 2005;493:167–76.
- [6] Bluhm RL, Williamson PC, Osuch EA, et al. Alterations in default network connectivity in posttraumatic stress disorder related to early-life trauma. *J Psychiatry Neurosci* 2009;34:187–94.
- [7] Lanius RA, Bluhm RL, Coupland NJ, et al. Default mode network connectivity as a predictor of post-traumatic stress disorder symptom severity in acutely traumatized subjects. *Acta Psychiatr Scand* 2010;121:33–40.
- [8] Du MY, Liao W, Lui S, et al. Altered functional connectivity in the brain default-mode network of earthquake survivors persists after 2 years despite recovery from anxiety symptoms. *Soc Cogn Affect Neurosci* 2015;10:1497–505.
- [9] Sripada RK, King AP, Welsh RC, et al. Neural dysregulation in posttraumatic stress disorder: evidence for disrupted equilibrium between salience and default mode brain networks. *Psychosom Med* 2012;74:904–11.
- [10] King AP, Block SR, Sripada RK, et al. Altered default mode network (DMN) resting state functional connectivity following a mindfulness-based exposure therapy for posttraumatic stress disorder (PTSD) in combat veterans of Afghanistan and Iraq. *Depress Anxiety* 2016;33:289–99.
- [11] Tursich M, Ros T, Frewen PA, et al. Distinct intrinsic network connectivity patterns of post-traumatic stress disorder symptom clusters. *Acta Psychiatr Scand* 2015;132:29–38.
- [12] Fornito A, Zalesky A, Breakspear M. Graph analysis of the human connectome: promise, progress, and pitfalls. *Neuroimage* 2013;80:426–44.
- [13] Lei D, Li K, Li L, et al. Disrupted functional brain connectome in patients with posttraumatic stress disorder. *Radiology* 2015;276:818–27.
- [14] Kennis M, van Rooij SJ, van den Heuvel MP, et al. Functional network topology associated with posttraumatic stress disorder in veterans. *Neuroimage Clin* 2015;10:302–9.
- [15] Suo X, Lei D, Li K, et al. Disrupted brain network topology in pediatric posttraumatic stress disorder: a resting-state fMRI study. *Hum Brain Mapp* 2015;36:3677–86.
- [16] Wang L, Li H, Liang Y, et al. Amnesic mild cognitive impairment: topological reorganization of the default-mode network. *Radiology* 2013;268:501–14.
- [17] Qi R, Ke J, Schoepf UJ, et al. Topological reorganization of the default mode network in irritable bowel syndrome. *Mol Neurobiol* 2016;53:6585–93.
- [18] Blanchard EB, Jones-Alexander J, Buckley TC, et al. Psychometric properties of the PTSD Checklist (PCL). *Behav Res Ther* 1996;34:669–73.
- [19] Blake DD, Weathers FW, Nagy LM, et al. The development of a Clinician-Administered PTSD Scale. *J Trauma Stress* 1995;8:75–90.
- [20] Jin C, Qi R, Yin Y, et al. Abnormalities in whole-brain functional connectivity observed in treatment-naive post-traumatic stress disorder patients following an earthquake. *Psychol Med* 2014;44:1927–36.
- [21] Trull TJ, Vergés A, Wood PK, et al. The structure of Diagnostic and Statistical Manual of Mental Disorders (4th edition, text revision) personality disorder symptoms in a large national sample. *Personal Disord* 2012;3:355–69.
- [22] Liao W, Chen H, Feng Y, et al. Selective aberrant functional connectivity of resting state networks in social anxiety disorder. *Neuroimage* 2010;52:1549–58.
- [23] Fox MD, Snyder AZ, Vincent JL, et al. The human brain is intrinsically organized into dynamic, anticorrelated functional networks. *Proc Natl Acad Sci U S A* 2005;102:9673–8.
- [24] Shiner WR, Ryali S, Rykhlevskaia E, et al. Decoding subject-driven cognitive states with whole-brain connectivity patterns. *Cereb Cortex* 2012;22:158–65.
- [25] Chang C, Liu Z, Chen MC, et al. EEG correlates of time-varying BOLD functional connectivity. *Neuroimage* 2013;72:227–36.
- [26] Bullmore E, Sporns O. Complex brain networks: graph theoretical analysis of structural and functional systems. *Nat Rev Neurosci* 2009;10:186–98.
- [27] He Y, Wang J, Wang L, et al. Uncovering intrinsic modular organization of spontaneous brain activity in humans. *PLoS One* 2009;4:e5226.
- [28] Latora V, Marchiori M. Efficient behavior of small-world networks. *Phys Rev Lett* 2001;87:198701.
- [29] Xia M, He Y. Magnetic resonance imaging and graph theoretical analysis of complex brain networks in neuropsychiatric disorders. *Brain Connect* 2011;1:349–65.
- [30] Watts DJ, Strogatz SH. Collective dynamics of 'small-world' networks. *Nature* 1998;393:440–2.
- [31] Zhang J, Wang J, Wu Q, et al. Disrupted brain connectivity networks in drug-naive, first-episode major depressive disorder. *Biol Psychiatry* 2011;70:334–42.
- [32] Wang T, Shi F, Jin Y, et al. Multilevel deficiency of white matter connectivity networks in Alzheimer's disease: a diffusion MRI study with DTI and HARDI models. *Neural Plast* 2016;2016:2947136.
- [33] Wang JH, Zuo XN, Gohel S, et al. Graph theoretical analysis of functional brain networks: test-retest evaluation on short- and long-term resting-state functional MRI data. *PLoS One* 2011;6:e21976.
- [34] Fornito A, Yoon J, Zalesky A, et al. General and specific functional connectivity disturbances in first-episode schizophrenia during cognitive control performance. *Biol Psychiatry* 2011;70:64–72.
- [35] Koch SB, van Zuiden M, Nawijn L, et al. Aberrant resting-state brain activity in posttraumatic stress disorder: a meta-analysis and systematic review. *Depress Anxiety* 2016;33:592–605.
- [36] Leech R, Sharp DJ. The role of the posterior cingulate cortex in cognition and disease. *Brain* 2014;137(Pt 1):12–32.
- [37] Bremner JD, Narayan M, Staib LH, et al. Neural correlates of memories of childhood sexual abuse in women with and without posttraumatic stress disorder. *Am J Psychiatry* 1999;156:1787–95.
- [38] Boccia M, D'Amico S, Bianchini F, et al. Different neural modifications underpin PTSD after different traumatic events: an fMRI meta-analytic study. *Brain Imaging Behav* 2016;10:226–37.
- [39] Giustino TF, Maren S. The role of the medial prefrontal cortex in the conditioning and extinction of fear. *Front Behav Neurosci* 2015;9:298.
- [40] Li L, Wu M, Liao Y, et al. Grey matter reduction associated with posttraumatic stress disorder and traumatic stress. *Neurosci Biobehav Rev* 2014;43:163–72.
- [41] Brohawn KH, Offringa R, Pfaff DL, et al. The neural correlates of emotional memory in posttraumatic stress disorder. *Biol Psychiatry* 2010;68:1023–30.
- [42] Hayes JP, LaBar KS, McCarthy G, et al. VISN 6 Mid-Atlantic MIRECC workgroup Reduced hippocampal and amygdala activity predicts memory distortions for trauma reminders in combat-related PTSD. *J Psychiatr Res* 2011;45:660–9.